The Astrophysical Journal, 773:32 (7pp), 2013 August 10 doi:10.1088/0004-637X/773/1/32

A LYMAN BREAK GALAXY IN THE EPOCH OF REIONIZATION FROM *HUBBLE SPACE TELESCOPE* GRISM SPECTROSCOPY

James E. Rhoads[1], Sangeeta Malhotra[1], Daniel Stern[2], Mark Dickinson[3], Norbert Pirzkal[4], Hyron Spinrad[5], Naveen Reddy[6], Nimish Hathi[7], Norman Grogin[4], Anton Koekemoer[4], Michael A. Peth[4,8], Seth Cohen[1], Zhenya Zheng[1], Tamas Budavari[8], Ignacio Ferreras[9], Jonathan P. Gardner[10], Caryl Gronwall[11], Zoltan Haiman[12], Martin Kümmel[13], Gerhardt Meurer[14], Leonidas Moustakas[2], Nino Panagia[4,15,16], Anna Pasquali[17], Kailash Sahu[4], Sperello di Serego Alighieri[18], Rachel Somerville[19], Amber Straughn[10], Jeremy Walsh[20], Rogier Windhorst[1], Chun Xu[21], and Haojing Yan[22]

[1] School of Earth and Space Exploration, Arizona State University, Tempe, AZ 85287, USA; James.Rhoads@asu.edu
[2] Jet Propulsion Laboratory, California Institute of Technology, 4800 Oak Grove Drive, Pasadena, CA 91109, USA
[3] National Optical Astronomy Observatory, Tucson, AZ, USA
[4] Space Telescope Science Institute, Baltimore, MD, USA
[5] University of California, Berkeley, CA, USA
[6] University of California, Riverside, CA, USA
[7] Observatories of the Carnegie Institution of Washington, Pasadena, CA, USA
[8] Johns Hopkins University, Baltimore, MD, USA
[9] Mullard Space Science Laboratory, University College London, Holmbury St Mary, Dorking, Surrey RH5 6NT, UK
[10] NASA Goddard Space Flight Center, Astrophysics Science Division, Observational Cosmology Laboratory, Code 665, Greenbelt, MD 20771, USA
[11] Department of Astronomy & Astrophysics, and Institute for Gravitation and the Cosmos, The Pennsylvania State University, University Park, PA 16802, USA
[12] Columbia University, New York, NY, USA
[13] Universitäts-Sternwarte München, Scheinerstr. 1, D-81679 München, Germany
[14] International Centre for Radio Astronomy Research, University of Western Australia, M468, 35 Stirling Highway, Crawley, WA 6009, Australia
[15] INAF–Osservatorio Astrofisico di Catania, Italy
[16] Supernova Ltd, OYV #131, Northsound Road, Virgin Gorda, VG1150, British Virgin Islands
[17] Astronomisches Rechen-Institut, Zentrum für Astronomie der Universität Heidelberg, Mönchhofstrasse 12–14, D-69120 Heidelberg, Germany
[18] INAF–Osservatorio Astrofisico di Arcetri, Italy
[19] Rutgers University, Piscataway, NJ, USA
[20] European Southern Observatory, Garching, Germany
[21] Shanghai Institute of Technical Physics, Shanghai, China
[22] Department of Physics and Astronomy, 223 Physics Bldg., University of Missouri, Columbia, MO 65211-7010, USA
Received 2013 February 28; accepted 2013 May 22; published 2013 July 22

ABSTRACT

We present observations of a luminous galaxy at $z = 6.573$—the end of the reionization epoch—which has been spectroscopically confirmed twice. The first spectroscopic confirmation comes from slitless *Hubble Space Telescope* Advanced Camera for Surveys grism spectra from the PEARS survey (Probing Evolution And Reionization Spectroscopically), which show a dramatic continuum break in the spectrum at rest frame 1216 Å. The second confirmation is done with Keck + DEIMOS. The continuum is not clearly detected with ground-based spectra, but high wavelength resolution enables the Lyα emission line profile to be determined. We compare the line profile to composite line profiles at $z = 4.5$. The Lyα line profile shows no signature of a damping wing attenuation, confirming that the intergalactic gas is ionized at $z = 6.57$. Spectra of Lyman breaks at yet higher redshifts will be possible using comparably deep observations with IR-sensitive grisms, even at redshifts where Lyα is too attenuated by the neutral intergalactic medium to be detectable using traditional spectroscopy from the ground.

Key words: galaxies: evolution – galaxies: formation – galaxies: high-redshift

Online-only material: color figures

1. INTRODUCTION

To properly understand the history of cosmic dawn, we must be able to reliably identify galaxies observed during the epoch of reionization. Such galaxies are the most likely sources of the radiation that ionized intergalactic hydrogen. They are the best places to look for signatures of primordial star formation: even if the buildup of heavy elements is rapid, the fraction of galaxies forming their first generations of stars should be higher if we observe them when the universe itself was young. The pace of their growth depends on incompletely understood physical processes—both the onset of star-formation in low-metallicity conditions, and the potential disruption of later star-formation by the ionizing radiation and/or supernovae produced by the first stellar generation. The best way to constrain the range of possible outcomes from these various processes is to take a direct, observational census of galaxies throughout the reionization era—from its end at $6 \lesssim z \lesssim 7$, back to the earliest galaxies we can identify.

Much progress has been made recently in this direction, due primarily to the dramatic increase in near-infrared imaging sensitivity and survey efficiency afforded by the Wide Field Camera 3 (WFC3) Infrared (IR) channel on the *Hubble Space Telescope* (*HST*). Imaging surveys with WFC3-IR have provided tens to hundreds of $z > 7$ galaxy candidates, identified by the Lyα absorption break in their broad band colors (e.g., Bouwens et al. 2010; Yan et al. 2010, 2012; Finkelstein et al. 2012). (We will refer to these as "Lyman break galaxies (LBGs)," while noting that selection by a strong continuum break can identify either the 912 Å break due to Lyman continuum absorption, or

the 1216 Å break due to Lyα absorption. Since the Lyα forest is optically thick for $z \gtrsim 5$, surveys for $z > 5$ galaxies use the Lyα absorption break, while those at $z \lesssim 3$ primarily identify the 912 Å break.) These broad band *HST* searches have broken new ground, primarily because the NIR sky is orders of magnitude darker in space. Alternative, ground-based search methods can find Lyα emitting galaxies efficiently at selected redshifts ($z =$ 6.5, 6.9, 7.3, 7.7, 8.8) where the line falls in dark windows in the night sky spectrum, using either narrow bandpass imaging (e.g., Hu et al. 2002, 2010; Rhoads et al. 2004, 2012; Iye et al. 2006; Willis et al. 2008; Ouchi et al. 2010; Hibon et al. 2010; Tilvi et al. 2010; Kashikawa et al. 2011; Clément et al. 2012; Shibuya et al. 2012; Krug et al. 2012), or direct spectroscopic searches (e.g., Kurk et al. 2004; Martin & Sawicki 2004; van Breukelen et al. 2005; Martin et al. 2008; Dressler et al. 2011).

However, issues remain. Ground-based near-IR spectroscopy can only confirm these objects easily when they have strong Lyα lines in clean regions of the night sky spectrum. Thus, while dozens have been confirmed up to $z = 6.5$ (Hu et al. 2010; Ouchi et al. 2010; Kashikawa et al. 2011), only a handful are confirmed at higher redshifts (Iye et al. 2006; Rhoads et al. 2012; Shibuya et al. 2012; Pentericci et al. 2011; Ono et al. 2012; Schenker et al. 2012). The crucial Lyα line may be rare and/or weak at redshifts where the intergalactic medium (IGM) was mostly neutral (and hence able to scatter Lyα photons). Meanwhile, sample contamination by foreground galaxies becomes an increasing worry at higher redshifts, where the volume available for such contaminants becomes large. Finally, the candidate lists from the highest redshift galaxy surveys can be disturbingly unstable, showing little overlap when different groups examine the same data, or even when the same group re-observes the same field (e.g., Yan et al. 2012; Oesch et al. 2012).

Slitless spectroscopy with the *HST* offers a solution to many of these issues. Space telescopes avoid the crippling effects of Earth's atmosphere on the near-IR sky. *HST*'s spatial resolution is well matched to the sizes of high redshift galaxies. These slitless grisms thus provide unmatched sensitivity to continuum emission from faint, compact high redshift galaxies.

Here we present PEARS-N-101687, which we identified as a $z \approx 6.6$ galaxy based on its Lyα break in deep Advanced Camera for Surveys (ACS) G800L slitless spectra from the PEARS survey (Probing Evolution And Reionization Spectroscopically). Our follow-up spectrum with Keck+DEIMOS confirms it at $z = 6.573$. This makes it only the second galaxy identified at such high redshift using *HST*'s slitless grisms, after UDF-30591 at $z \approx 6.7$ (Malhotra et al. 2005), and the first at this redshift with both *HST* and ground-based redshifts. While the sensitivity of the ACS grism declines beyond 9600 Å, the WFC3 IR channel has a similar grism and can perform spectroscopic confirmations at even higher redshifts.

We organize the paper as follows. In Section 2, we describe the PEARS survey observations and data analysis. In Section 3, we present follow-up spectroscopy at higher spectral resolution from the Keck telescope. In Section 4, we discuss the implications of our findings for the field of high-redshift galaxy searches. We conclude in Section 5. Most photometry discussed here is from the *HST*-GOODS survey (Giavalisco et al. 2004). We denote the GOODS filters F450W as "B_{450}," F606W as "V_{606}," F775W as "i_{775}," and F850LP as "z_{850}," and use the AB magnitude system. Throughout the paper, we adopt a Λ-CDM "concordance cosmology" with $\Omega_M = 0.27$, $\Omega_\Lambda = 0.73$, and $H_0 = 71$ km s^{-1} Mpc^{-1} (see Spergel et al. 2007).

2. PEARS GRISM OBSERVATIONS

PEARS is the most extensive systematic survey conducted with the G800L grism on the *HST's* ACS Wide Field Camera (ACS-WFC). PEARS is an *HST* Treasury program led by S. Malhotra (program ID HST-GO-10530). It covers a total of nine fields, including one deep pointing in the Hubble Ultra Deep Field (HUDF), and eight wide-field pointings (four each in the GOODS-North and GOODS-South regions). Each pointing was observed at three or four distinct roll angles to mitigate the impact of overlap between spectra of nearby objects.

The *HST* slitless spectra were reduced using the aXe package (Kümmel et al. 2009), closely following the procedure used for the earlier GRism ACS Program for Extragalactic Science survey (Pirzkal et al. 2004). For each roll angle, the relative offsets of all exposures were determined using zero-order images and narrow emission lines. The data for each roll angle were ultimately combined into two-dimensional (2D) spectroscopic stacks and extracted one-dimensional (1D) spectra for each source and each observed position angle.

To identify and spectroscopically confirm the highest redshift LBGs in the survey, we followed a procedure based on Malhotra et al. (2005). We started with the GOODS v1.9 images and performed our own SExtractor photometry. We then applied a "liberal" *i*-dropout criterion to generate a list of candidate LBGs. Since the GOODS data do not include observations redder than *z*-band (and our candidate selection was done prior to the installation of WFC3), this ultimately amounts to using $i_{775} - z_{850} > 0.9$ mag. For each of these objects, we calculated the net significance ("netsig") parameter $\mathcal{N}$ (Pirzkal et al. 2004) to determine which spectra might have sufficient information for a redshift measurement. ("Netsig" is defined by first sorting all pixels in a spectrum in descending order of signal-to-noise ratio; calculating the signal-to-noise ratio S_n obtained by combining flux from the brightest n pixels, for all n between 1 and the total number of pixels in the spectrum; and finally taking $\mathcal{N} = \max\{S_n\}$.)

After selecting candidates by $(i-z)$ color and ranking them by netsig, several PEARS team members (including S.M., J.E.R., N.P., S.C., and N.G.) examined the spectra by eye. We did this because a straight $(i - z)$ color cut can select extremely red objects (EROs) as well as LBGs, but the spectral signatures of the two are distinct. (EROs show a smooth rise toward the red, while LBGs at these redshifts show a step function at the redshifted wavelength of Lyα forest absorption.)

The highest redshift object identified in the PEARS-Wide fields through this process was the galaxy PEARS-N-101687, at equatorial coordinates 12:37:25.65 +62:17:43.5 (J2000). This object has magnitude $z_{850} = 26.16$ mag, while it is undetected in the B_{450}, V_{606}, and i_{775} bands. Its grism redshift estimate is $z = 6.6 \pm 0.1$ based on the observed location of the Lyα break. We show postage stamp images of the object from the GOODS data in Figure 1, and the 2D PEARS spectrum in Figure 2.

3. KECK FOLLOW-UP OBSERVATIONS

We selected several galaxies, including PEARS-N-101687, for follow-up observations during a Keck observing run of three half nights on UT 2007 April 13–15, using the DEep Imaging Multi-Object Spectrograph (DEIMOS; Faber et al. 2003). These observations were part of a program of a deep field followup led by Spinrad, Stern, and Dickinson, using Keck telescope time from the University of California system. PEARS-N-101687 was included on three slit masks during this run, and also on one

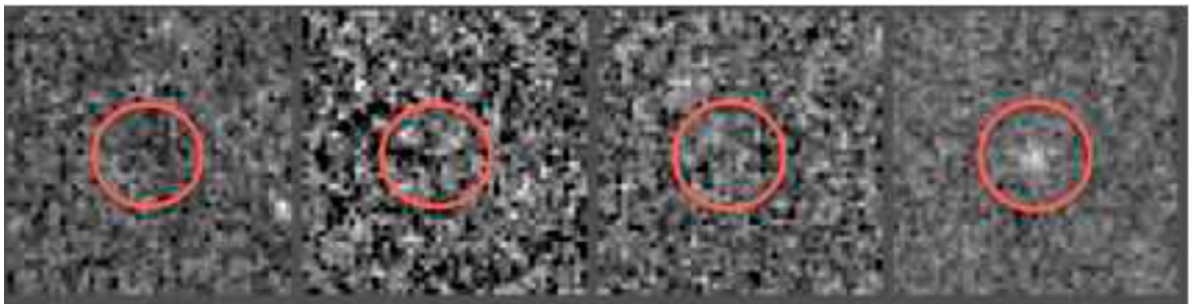

Figure 1. Direct imaging of PEARS-N-101687 from the GOODS survey (Giavalisco et al. 2004). The object is effectively undetected in the B_{450}, V_{606}, and i_{775} bands (left three panels), while it is clearly seen in the z_{850} band (right panel) with magnitude $z_{850} = 26.16$ (AB). Each panel is $1\farcs5 \times 1\farcs5$ in size.

(A color version of this figure is available in the online journal.)

Table 1
Log of DEIMOS Observations of PEARS-N-101687

Mask	Obs Dates (UT)	$N_{\rm exp}\times$ Duration	Total Time	Conditions	Comments
hdf07c	2007 Apr 14	4×1800 s	7200 s	Clear, $>1''$ seeing	Good
hdf07d	2007 Apr 14–15	5×1800 s	9000 s	Clear, $>1''$ seeing	Good
hdf07e	2007 Apr 16	2820 s	2820 s	Clear, $1\farcs4$ seeing	Not useful
hdf08a	2008 Mar 6	$6 \times \sim 1800$ s	10500 s		Good

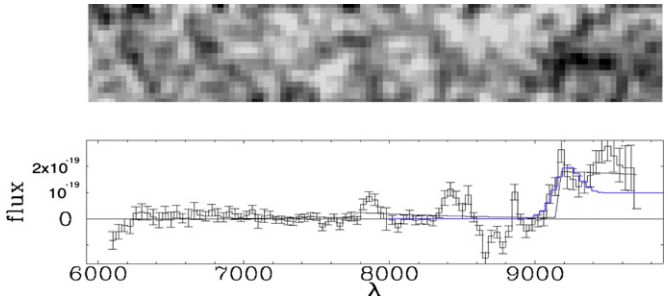

Figure 2. Upper: the 2D PEARS spectrum of PEARS-N-101687, displayed in inverse video (dark = more flux), with all three position angles coadded and with a 2 pixel ($0\farcs1 \times 80$ Å) FWHM smoothing applied. A short segment of continuum is evident, with a blue edge near 9230 Å due to the Lyα forest break, and a red cutoff imposed by the falloff of instrumental efficiency. Lower: a 1D extraction of the PEARS spectrum, in erg cm^{-2} s^{-1} Å^{-1}. The thin black curve is a best-fitting continuum + IGM absorption model with redshift $z = 6.6$ and a continuum level of AB = 25.7 mag on the red side of the Lyα break. The blue curve is a model based on the line flux from the Keck spectrum, and the continuum flux level and line spread function width expected based on *HST* imaging.

(A color version of this figure is available in the online journal.)

additional mask observed in early 2008. All observations used the 600 line grism. The observations are summarized briefly in Table 1.

We show the extracted Keck + DEIMOS spectrum of PEARS-N-101687 in Figure 3. The galaxy shows a prominent Lyα line at redshift $z = 6.573$, consistent with the grism-based redshift of $z = 6.6 \pm 0.1$. This line is plainly detected in each of the three masks that have >1 hr of exposure time. Averaging the spectra from the three useful masks together yields a better detection of the asymmetric line, along with hints of the continuum on the red side of the line. No other emission features are convincingly present in the DEIMOS spectrum, which spans approximately $5000\,\text{Å} < \lambda < 10000\,\text{Å}$.

To estimate the spectroscopic line flux, we first calibrated the observed spectra using a DEIMOS sensitivity function derived for the same grism but on another night. To compensate for differences in throughput (e.g., due to differences in slit losses or atmospheric extinction between nights), we identified two objects in the 2008 mask with reasonably bright continuum flux ($i_{775} \sim 21$–22 mag). For each, we weighted the spectrum by the throughput of the *HST* ACS F775W filter, integrated, and compared the result to the broad band photometry from the GOODS project. This yielded a mean correction of about 30%, relative to our archival sensitivity function. The reference objects used are both galaxies at moderate redshift, and although they are not point sources, they are considerably smaller than the DEIMOS slit. We measured their fluxes in a virtual $1''$ slit in ACS images both before and after smoothing with a $1''$ Gaussian "seeing." We thereby found that differential slit losses would require a 10% correction to the spectroscopic flux of a point source. Applying our calibration to the spectrum of PEARS-N-101687 (and assuming the source is point-like in $1''$ seeing), we find a spectroscopic line flux of $f_{\rm Ly\alpha} \approx (2.8 \pm 0.6) \times 10^{-17}$ erg cm^{-2} s^{-1}, where the uncertainty is dominated by the flux calibration of the spectrum.

4. DISCUSSION

4.1. Other Observations of PEARS-N-101687

While no spectrum of PEARS-N-101687 appears to have been previously published, the object is listed as Lyα candidate in Hu et al. (2010, Table 3, second entry), based on a narrowband excess in a filter with 9210 Å central wavelength and 120 Å FWHM. The narrowband magnitude published in that work, AB = 24.36 mag, corresponds to a total flux of about 2.75×10^{-17} erg cm^{-2} s^{-1} within the 120 Å filter.

The CANDELS survey (Grogin et al. 2011; Koekemoer et al. 2011) provides WFC3-IR photometry of this region. PEARS-N-101687 is detected at high confidence in the near infrared. CANDELS catalog magnitudes for the source are $z_{850} = 26.36 \pm 0.18$, $Y_{105} = 25.27 \pm 0.11$, $J_{125} = 25.11 \pm 0.09$, and $H_{160} = 25.04 \pm 0.08$ mag. (Note the small [0.2 mag, 1σ] difference between our previous z_{850} photometry and the CANDELS project photometry.) The Y_{105} magnitude is near the wavelength of the Lyα line, but unaffected by Lyα forest

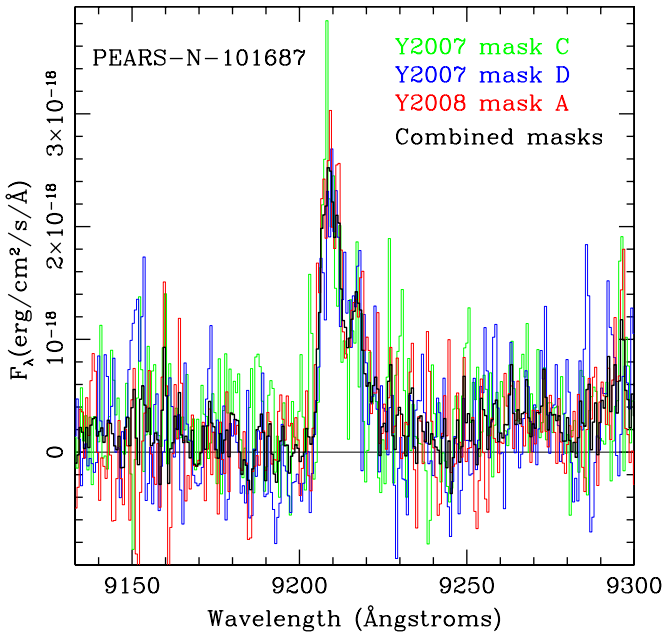

Figure 3. The 1D Keck + DEIMOS spectrum of PEARS-N-101687. The prominent line at 9210 Å is identified as Lyα based on the strong break at 9210 Å in the *HST* PEARS grism spectrum, the complete absence of flux blueward of the line, and the prominent asymmetry of the line. The spectrum from each individual deep Keck+DEIMOS data set is shown with its own color, and the exposure-time weighted mean of these three masks is shown in black. The spectra are flux calibrated (with $\sim \pm 20\%$ accuracy) as described in the text. There is a suggestion of continuum flux on the red side of the line in the sum of all the Keck data. No other convincing features are seen in the full DEIMOS spectrum, which fully covers the range 5000–10000 Å.

absorption. Using the Y_{105} magnitude to estimate the continuum flux density just redward of the Lyα line, we expect $\approx 6 \times 10^{-18}$ erg cm^{-2} s^{-1} of continuum flux in the narrowband filter used by Hu et al. (2010). This leaves $\sim 2.1 \times 10^{-17}$ erg cm^{-2} s^{-1} as the expected line flux based on photometry. This is 25% below the flux we derive from the Keck DEIMOS observations, but consistent within the combined uncertainties of all the data sets involved.

4.2. Comparison of Grism and Slit Spectra

The galaxy PEARS-N-101687 is reminiscent of the bright $z = 5.83$ dropout galaxy UDF2225 (Malhotra et al. 2005) = SiD2 (Dickinson et al. 2004) = SBM3 (Stanway et al. 2003, 2004), in that the ACS grism spectrum shows a clear continuum with a Lyman break, while the follow-up slit spectrum from Keck shows a prominent Lyα line. This contrast is a consequence of the differing capabilities of the two instruments. The high spatial resolution and low sky background of *HST* + ACS provide exquisite sensitivity to faint continuum emission. On the other hand, the higher spectral resolution of Keck+DEIMOS slit spectra provides a clearer look at the Lyα line. The PEARS ACS spectrum does have sufficient sensitivity to detect the observed Lyα line, but the line is blended with the Lyman break at the resolution of the grism. For the Lyα line to appear obvious at $z \gtrsim 5$, where the Lyα forest is optically thick, its observer-frame equivalent width must exceed the instrumental resolution, which is about 150–200 Å for PEARS-N-101687 (based on its half-light diameter in the GOODS images). The observed equivalent width is modestly larger than this threshold, but not so large that the line is expected to be prominent in the grism spectrum. The 2D *HST* spectrum also shows a hint of extended Lyα emission (see Rhoads et al. 2009; Bond et al. 2010; Finkelstein et al. 2011), which would lie outside the extraction region for PEARS 1D spectra, but within the wider Keck slit, further increasing the relative prominence of the line in the Keck spectrum.

We have modeled the expected 1D grism spectrum by assuming a flat continuum at the level of the Y_{105} flux measurement, a Lyα line at the wavelength and flux observed by Keck, and a line spread function determined by the observed z_{850} angular size of the object and the dispersion of the ACS G800L grism. The resulting model is shown as a blue curve in Figure 2. Near the Lyα line, from 9000 to 9400 Å, the agreement is quite good. The largest discrepancy is at yet redder wavelengths, where the grism spectrum continuum appears to be above the Y_{105} flux. This may be due to an edge effect always present in flux-calibrated slitless spectra of extended sources. The counts at a particular pixel include redder light from one edge of the source, and bluer light from the other edge, but all counts in the pixel are converted to flux density using a single system throughput, which is the one appropriate for light from the centroid of the source that is dispersed onto that pixel. Where the efficiency is changing rapidly with wavelength, as it does in the 9500 Å region for the ACS/WFC, the net effect is an overestimate of the red flux. (Bumps in the 1D ACS spectrum at 7850 Å and 8400 Å could be contamination by other fainter sources, transmissive gaps in the OH forest absorption, or simply regions of somewhat correlated noise in the extracted spectrum.)

4.3. PEARS-N-101687 in Context

The galaxy PEARS-N-101687 is, for its redshift, a moderately bright object. It has a 1500 Å absolute magnitude $M_{1500} = -21.38$ mag, based on an interpolation of the CANDELS Y_{105} and J_{125} fluxes. Compared to the published luminosity function for a sample of candidate $z \approx 6.6$ LBGs from Bouwens et al. (2011), PEARS-N-101687 is about 3× (or 1.25 mag) brighter than L^* (the characteristic galaxy luminosity for the best fit Schechter function).

The Lyα luminosity of PEARS-N-101687 is $L_{\mathrm{Ly}\alpha} = 1.4 \times 10^{43}$ erg s^{-1}, based on its line flux from the DEIMOS spectrum and a "concordance" cosmology luminosity distance of $d_L = 65.5$ Gpc. This is on the bright end of the distribution for $z = 6.5$ narrowband-selected Lyα galaxy samples, which yield Schechter function fits with characteristic luminosities of $L_* = 4.4 \times 10^{42}$, 5.8×10^{42}, and 1.0×10^{43} erg s^{-1}, respectively, for Ouchi et al. (2010), Kashikawa et al. (2011), and Hu et al. (2010).

The spectroscopic line flux of PEARS-N-101687, combined with its Y_{105} flux density, yields an observer frame equivalent width of EW $= 290 \pm 80$ Å, or in the rest frame, EW$_0$ $= 38 \pm 12$ Å. This is below the average for narrowband-selected samples, as one might expect given that we identified the object by its continuum trace in the PEARS spectrum. Lyα galaxies often have rest frame equivalent widths above 200 Å (Malhotra & Rhoads 2002), and at $z = 6.5$, over 75% of the narrowband selected Lyα emitters have EW$_0$ > 40 Å (Kashikawa et al. 2011; Ouchi et al. 2010).

The Lyα line asymmetry in PEARS-N-101687 is prominent, even by the standards of high redshift Lyα emitting galaxies. Using the asymmetry measures[23] from Rhoads et al. (2003), we

[23] These are $a_\lambda = (\lambda_{10,r} - \lambda_p)/(\lambda_p - \lambda_{10,b})$ and $a_f = \int_{\lambda_p}^{\lambda_{10,r}} f_\lambda d\lambda / \int_{\lambda_{10,b}}^{\lambda_p} f_\lambda d\lambda$. Here λ_p is the wavelength where the line peaks, and $\lambda_{10,b}$ and $\lambda_{10,r}$ are the wavelengths where the flux falls to 10% of peak on the blue and red sides of the line.

find $a_\lambda = 3.59$ and $a_f = 3.47$. Comparing these to a sample of 58 Lyα emitters observed using the same spectrograph and grating (Dawson et al. 2007), PEARS-N-101687 has the largest value of a_f, and the fifth-largest value of a_λ. This may be partly due to Lyα forest absorption of flux on the blue side of the systemic velocity, since the Lyα forest optical depth at $z = 6.57$ will exceed that at the lower redshift ($z = 4.5$) sample of Dawson et al. (2007).

In addition to its asymmetry, the line profile shows a dip at 9214 Å, separating a secondary peak (at 9217 Å) from the primary one (at 9207 Å). The dip is about 4 Å wide; the flux density there drops by about 40% relative to a smoothed "envelope" of the line flux; and the feature is significant at about the 3σ level. Such a feature could be explained by neutral gas in front of the emitter; two distinct emitting regions; or some more complex interplay of Lyα emission and scattering in a moving medium. If we interpret the dip as absorption, we can estimate the equivalent width and column density of the absorber by interpolating across the dip (from 9211.5 Å to 9217 Å). This yields an equivalent width of -1.8 Å (observer-frame) or -0.24 Å (rest frame; here the "$-$" sign indicates absorption). The maximum optical depth is 0.6, and the system is 100 km s^{-1} wide (FWHM in optical depth). The required column density is only 4×10^{13} cm^{-2} of neutral gas—comparable to a Lyα forest absorber, though with a greater velocity width. The superimposition of this absorption on the red part of the emission line would suggest an infalling gas cloud in the neighborhood of PEARS-N-101687.

If we instead interpret the feature as additional emission at 9217 Å, the corresponding line flux is 2×10^{-18} erg cm^{-2} s^{-1}. This could correspond to a *faint* Lyα galaxy along the line-of-sight to PEARS-N-101687, with a redshift of 6.582 (330 km s^{-1} redder than PEARS-N-101687 itself). This would require a projected separation of $\lesssim$2 kpc between PEARS-N-101687 and the putative interloper, since there is no visible evidence of a double morphology in the *HST* imaging. The line-of-sight separation could be much larger—a reasonable fraction of $\Delta v/H(z) \sim 400$ kpc. Thus, the "neighboring galaxy" hypothesis requires precise alignment along the line-of sight. We prefer instead either the absorber hypothesis, other radiative transfer effects internal to PEARS-N-101687, or perhaps just a $\sim 3\sigma$ statistical fluke in the spectroscopic observations.

4.4. Implications for Reionization

We have compared the spectrum of PEARS-N-101687 to a comparison sample of Lyα emitting galaxies at redshift $z = 4.5$ (Dawson et al. 2007). We selected these comparison spectra because they were obtained with the same instrument. We first constructed a composite Lyα line spectrum, by multiplicatively rescaling both the flux densities and wavelengths of individual galaxies' spectra to a common peak, and then computing both the mean and variance at each pixel.

We plot both the composite $z = 4.5$ Lyα spectrum and the Keck spectrum of in Figure 4. The agreement between the line profiles is remarkably good, apart from the dip/bump feature discussed above. Such agreement between $z \approx 6.57$ and $z = 4.5$ would be destroyed by the damping wing of Lyα if the IGM around PEARS-N-101687 were significantly neutral (see, e.g., Figure 5 of Jensen et al. 2013).

This conclusion is also supported by Lyα luminosity function arguments. Between one and three Lyα emitting galaxies as bright as PEARS-N-101687 might be expected in the $z > 6$ PEARS survey volume. If we posit attenuation of the Lyα line by 50%, however, as expected for neutral fractions $\gtrsim$50% (e.g., Haiman 2002; Jensen et al. 2013), the intrinsic line luminosity doubles. Then, the expected number of galaxies plummets to $\sim$0.15 in the full PEARS survey volume.

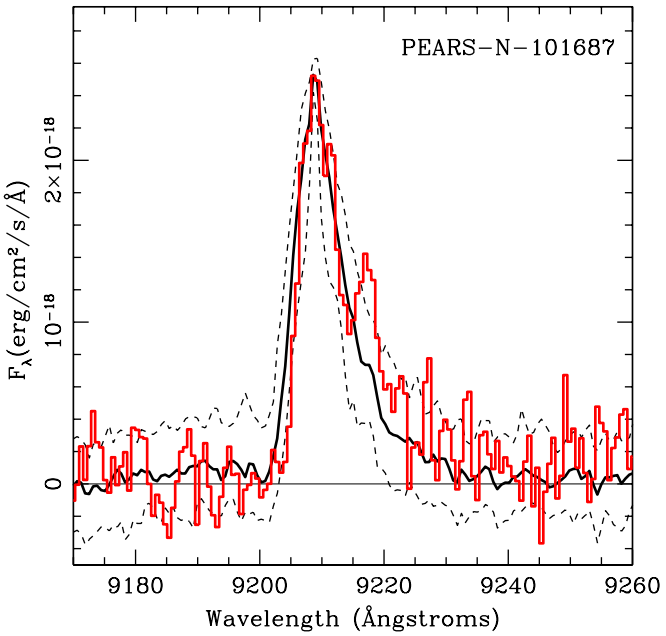

Figure 4. The 1D Keck + DEIMOS spectrum of PEARS-N-101687 (red histogram) is plotted atop the composite spectrum of $\sim$70 Lyα galaxies at redshift $z \approx 4.5$ (Dawson et al. 2007). The heavy black line shows the composite spectrum, while the dotted black lines enclose the $\pm 1\sigma$ range for individual spectra. The similarity of the PEARS-N-101687 spectrum to the $z \approx 4.5$ composite argues against major differences in the IGM ionization state between $z = 4.5$ and $z = 6.5$. In particular, the sharp cutoff at the blue edge of the peak would be hard to reconcile with the damping wing of neutral intergalactic gas.
(A color version of this figure is available in the online journal.)

4.5. The Need for Spectroscopy

Samples of well over 100 Lyman break selected galaxy candidates have now been published for photometric redshifts $z > 7$, based on the combination of deep photometry at optical and near-IR wavelengths using *HST* (e.g., Bouwens et al. 2010; Yan et al. 2010, 2012; Finkelstein et al. 2012). This represents substantial progress in understanding galaxy evolution around the end of the reionization era. However, essentially all these objects remain candidates at the moment, unconfirmed by spectroscopy. Deep grism spectra from *HST* can play a unique role in fixing this.

The overlap between samples published by different groups can be distressingly small, even when those groups use exactly the same data sets. For example, consider recent publications on the bright end of the $z \approx 8$ LBG luminosity function by Yan et al. (2012) and Oesch et al. (2012), both using the first epoch of the CANDELS deep observations of the GOODS-S region. The two groups publish eight and nine candidate galaxies, respectively. However, only two objects are identified by both papers. Similar levels of inconsistency have been frequent in earlier studies. Indeed, a recent paper by Ellis et al. (2013) reports that no previously published galaxy candidate at $8.5 < z < 10$ in the HUDF remains a viable high-redshift object after the addition of deeper imaging in the WFC3-IR F105W ("Y_{105}") and F140W ("JH_{140}") filters, while reporting a set of seven new candidates in that redshift range.

Several factors contribute to unreliable candidate lists. First, candidates are generally sought down to the limit of the survey depth, and objects near the faint limit of the data will then inevitably outnumber brighter, better measured sources. This means that photometric noise can push a galaxy across the selection line—in or out of a candidate sample, either in brightness or in color. Apparently minor differences in the choice of photometry method (apertures of various radii versus SExtractor "magauto", different methods of sky background estimation, etc.) can thus change samples appreciably.

Additionally, different authors may choose somewhat different criteria in selecting their candidates. Some use photometric redshifts (Finkelstein et al. 2012), while most others use straight color and magnitude cuts (e.g., Bouwens et al. 2010; Oesch et al. 2012; Yan et al. 2012), but the adopted color cuts are not always the same.

As the search redshift increases, the volume of foreground space and the variety of possible foreground contaminants also increases. For galaxies at $z > 7$, plausible foreground contaminants include Galactic brown dwarfs, and both early-type galaxies and ultra-strong emission line sources at intermediate redshifts (e.g., the candidate lensed $z = 11$ galaxy A2667-J1, whose spectrum revealed it to be an [O III]λλ4959,5007 emitter at $z = 2.082$; Hayes et al. 2012). While published $z > 7$ candidates usually have spectral energy distributions that are less well fit by any foreground model than by a LBG at $z > 7$, a majority allow viable $z \ll 7$ solutions. Recently, Pirzkal et al. (2013) have carried out an analysis of redshift estimation based on Markov Chain Monte Carlo fitting for samples of $z > 8$ galaxy candidates from the HUDF. They estimate that there is an average probability of 21% that these sources are low redshift interlopers.

Spectroscopic followup of $z > 7$ candidates can resolve these uncertainties. Ground-based spectra can confirm true $z > 7$ galaxies, but generally only when they have strong Lyα emission that is neither blocked by atmospheric H_2O absorption nor blended with strong OH airglow lines at the resolution of the spectrograph. Likewise, ground-based spectra may definitively rule out foreground objects whose Lyman break colors are due to strong emission lines in one or two filters.

However, sources without strong emission lines require continuum spectroscopy for definitive confirmation. For redshifts $z < 6$, a minority of LBGs have strong Lyα emission (Steidel et al. 2000; Stark et al. 2010). As we push to higher redshifts, within the epoch of reionization, Lyα will be obscured by resonant scattering in an increasingly neutral IGM (Miralda-Escude & Rees 1998; Haiman & Spaans 1999; Rhoads & Malhotra 2001). This effect offers valuable tests of reionization (e.g., Malhotra & Rhoads 2004; Stern et al. 2005; Pentericci et al. 2011; Ono et al. 2012; Schenker et al. 2012). It also means that continuum break spectroscopy is crucial for spectroscopic confirmations in the epoch of neutral gas.

Such spectroscopy is impractical from the ground with current instruments. From space, the absence of OH emission lines and water absorption makes the job much easier. To obtain a Lyman break confirmation at the knee of the luminosity function (L^*), we need to detect the continuum with good statistical significance, over a wavelength range of several hundred angstrom on the red side of the Lyman break. Another way to test the IGM neutral fraction is to look for evolution in the fraction of LBGs that show Lyα line emission (e.g., Stark et al. 2010). Multiple groups have studied this with small sample sizes, and find some evidence for a decreasing fraction at $z \geqslant 7.0$ (Pentericci et al. 2011; Schenker et al. 2012; Caruana et al. 2012) though the conclusions of Ono et al. (2012) are more ambiguous. A significant concern here is that *only* the Lyα emitting galaxies have so far been confirmed spectroscopically. The candidate galaxies not confirmed with a Lyα line will include those that lack line emission, but could also include cases where a Lyα line is hidden behind atmospheric H_2O absorption or OH emission features, or interlopers that are not actually high-redshift sources at all. Thus when the Lyα fraction is reported the denominator of high-z galaxies is itself in doubt. The papers discussed above make statistical corrections to account for these effects, but such corrections require an exquisite understanding of photometric redshift uncertainties. Space grism spectroscopy can provide direct spectroscopic confirmation based on continuum break. Deep integrations with *HST* grisms can accomplish this, spectroscopically confirming redshifts for objects as faint as the 27th magnitude (this work; Malhotra et al. 2005; Rhoads et al. 2009).

5. SUMMARY/CONCLUSIONS

We present here PEARS-N-101687, the highest redshift galaxy identified in the wide-field component of the PEARS slitless spectroscopic survey, which achieved a depth of 20 orbits of *HST* ACS G800L slitless spectroscopy over 80 arcmin^2. Its grism redshift, $z = 6.6 \pm 0.1$, is the second highest redshift ever reported from *HST* slitless spectroscopy, after UDF-30591 at $z = 6.7$ (Malhotra et al. 2005). While galaxies substantially fainter than PEARS-N-101687 have been spectroscopically confirmed at the sensitivity limit of our ACS slitless spectroscopy in the HUDF, the wavelength limit of the ACS WFC CCD detectors effectively limits the survey redshifts to $z \lesssim 6.7$ (Malhotra et al. 2005).

Keck telescope + DEIMOS followup of this object confirms and refines its grism redshift: $z = 6.573$. The object has a rest-frame UV continuum magnitude $M_{1500} = -21.38$ mag, a Lyα line luminosity of 1.4×10^{43} erg s^{-1}, and a rest-frame equivalent width of 38 ± 12 Å. This makes it a relatively luminous Lyα emitting LBG. We emphasize that the discovery and redshift from *HST* PEARS are based primarily on the continuum and Lyα forest break, and not on the Lyα emission line, which is not prominent in the *HST* spectrum. The Keck spectrum closely matches the composite spectrum of $z \approx 4.5$ Lyα emitting galaxies. In particular, it shows no evidence for additional absorption at the blue edge of the line, as would be expected in a significantly neutral IGM. We therefore conclude that reionization is essentially complete at $z \approx 6.6$ in the neighborhood of PEARS-N-101687.

The discovery of this object demonstrates the value of deep continuum observations with *HST* slitless grisms for spectroscopic confirmation of galaxies in the epoch of reionization. Comparably sensitive observations with the *HST* WFC3-IR channel grisms have the potential to provide Lyman break spectroscopic confirmations of $z > 7$ galaxies—something that still eludes our other observational capabilities, and that now presents a large obstacle in advancing our understanding of galaxy evolution in the era of cosmic dawn.

J.E.R. and S.M. thank the DARK Cosmology Centre and Nordea-fonden in Copenhagen, Denmark, and Anri's Place in Betalbatim, India, for hospitality during the completion of this work. We thank Mauro Giavalisco and the GOODS team for providing early access to GOODS v1.9 and v2.0 images

to help with spectroscopic extractions. We thank Emanuele Daddi for his contributions to the PEARS project. This work has been supported by grant HST-GO-10530 from STScI, which is operated by AURA for NASA under contract NAS 5-26555. The work of D.S. was carried out at the Jet Propulsion Laboratory, California Institute of Technology, under a contract with NASA. The Institute for Gravitation and the Cosmos is supported by the Eberly College of Science and the Office of the Senior Vice President for Research at the Pennsylvania State University. Some data presented herein were obtained at the W. M. Keck Observatory. The Observatory was made possible by the generous financial support of the W. M. Keck Foundation. The authors recognize and acknowledge the very significant cultural role and reverence that the summit of Mauna Kea has always had within the indigenous Hawaiian community. We are most fortunate to have the opportunity to conduct observations from this mountain.

REFERENCES

Bond, N. A., Feldmeier, J. J., Matković, A., et al. 2010, ApJL, 716, L200
Bouwens, R. J., Illingworth, G. D., Oesch, P. A., et al. 2010, ApJL, 709, L133
Bouwens, R. J., Illingworth, G. D., Oesch, P. A., et al. 2011, ApJ, 737, 90
Caruana, J., Bunker, A. J., Wilkins, S. M., et al. 2012, MNRAS, 427, 3055
Clément, B., Cuby, J.-G., Courbin, F., et al. 2012, A&A, 538, A66
Dawson, S., Rhoads, J. E., Malhotra, S., et al. 2007, ApJ, 671, 1227
Dickinson, M., Stern, D., Giavalisco, M., et al. 2004, ApJL, 600, L99
Dressler, A., Martin, C. L., Henry, A., Sawicki, M., & McCarthy, P. 2011, ApJ, 740, 71
Ellis, R. S., McLure, R. J., Dunlop, J. S., et al. 2013, ApJL, 763, L7
Faber, S. M., Phillips, A. C., Kibrick, R. I., et al. 2003, Proc. SPIE, 4841, 1657
Finkelstein, S. L., Cohen, S. H., Windhorst, R. A., et al. 2011, ApJ, 735, 5
Finkelstein, S. L., Papovich, C., Salmon, B., et al. 2012, ApJ, 756, 164
Giavalisco, M., Ferguson, H. C., Koekemoer, A. M., et al. 2004, ApJL, 600, L93
Grogin, N. A., Kocevski, D. D., Faber, S. M., et al. 2011, ApJS, 197, 35
Haiman, Z. 2002, ApJL, 576, L1
Haiman, Z., & Spaans, M. 1999, ApJ, 518, 138
Hayes, M., Laporte, N., Pelló, R., Schaerer, D., & Le Borgne, J.-F. 2012, MNRAS, 425, L19
Hibon, P., Cuby, J.-G., Willis, J., et al. 2010, A&A, 515, A97
Hu, E. M., Cowie, L. L., Barger, A. J., et al. 2010, ApJ, 725, 394
Hu, E. M., Cowie, L. L., McMahon, R. G., et al. 2002, ApJL, 568, L75
Iye, M., Ota, K., Kashikawa, N., et al. 2006, Natur, 443, 186
Jensen, H., Laursen, P., Mellema, G., et al. 2013, MNRAS, 428, 1366
Kashikawa, N., Shimasaku, K., Matsuda, Y., et al. 2011, ApJ, 734, 119
Koekemoer, A. M., Faber, S. M., Ferguson, H. C., et al. 2011, ApJS, 197, 36
Krug, H. B., Veilleux, S., Tilvi, V., et al. 2012, ApJ, 745, 122
Kümmel, M., Walsh, J. R., Pirzkal, N., Kuntschner, H., & Pasquali, A. 2009, PASP, 121, 59
Kurk, J. D., Cimatti, A., di Serego Alighieri, S., et al. 2004, A&A, 422, L13
Malhotra, S., & Rhoads, J. E. 2002, ApJL, 565, L71
Malhotra, S., & Rhoads, J. E. 2004, ApJL, 617, L5
Malhotra, S., Rhoads, J. E., Pirzkal, N., et al. 2005, ApJ, 626, 666
Martin, C. L., & Sawicki, M. 2004, ApJ, 603, 414
Martin, C. L., Sawicki, M., Dressler, A., & McCarthy, P. 2008, ApJ, 679, 942
Miralda-Escude, J., & Rees, M. J. 1998, ApJ, 497, 21
Oesch, P. A., Bouwens, R. J., Illingworth, G. D., et al. 2012, ApJ, 759, 135
Ono, Y., Ouchi, M., Mobasher, B., et al. 2012, ApJ, 744, 83
Ouchi, M., Shimasaku, K., Furusawa, H., et al. 2010, ApJ, 723, 869
Pentericci, L., Fontana, A., Vanzella, E., et al. 2011, ApJ, 743, 132
Pirzkal, N., Rothberg, B., Ryan, R., et al. 2013, ApJ, in press (arXiv:1304.4594)
Pirzkal, N., Xu, C., Malhotra, S., et al. 2004, ApJS, 154, 501
Rhoads, J. E., Dey, A., Malhotra, S., et al. 2003, AJ, 125, 1006
Rhoads, J. E., Hibon, P., Malhotra, S., Cooper, M., & Weiner, B. 2012, ApJL, 752, L28
Rhoads, J. E., & Malhotra, S. 2001, ApJL, 563, L5
Rhoads, J. E., Malhotra, S., Pirzkal, N., et al. 2009, ApJ, 697, 942
Rhoads, J. E., Xu, C., Dawson, S., et al. 2004, ApJ, 611, 59
Schenker, M. A., Stark, D. P., Ellis, R. S., et al. 2012, ApJ, 744, 179
Shibuya, T., Kashikawa, N., Ota, K., et al. 2012, ApJ, 752, 114
Spergel, D. N., Bean, R., Doré, O., et al. 2007, ApJS, 170, 377
Stanway, E. R., Bunker, A. J., & McMahon, R. G. 2003, MNRAS, 342, 439
Stanway, E. R., Bunker, A. J., McMahon, R. G., et al. 2004, ApJ, 607, 704
Stark, D. P., Ellis, R. S., Chiu, K., Ouchi, M., & Bunker, A. 2010, MNRAS, 408, 1628
Steidel, C. C., Adelberger, K. L., Shapley, A. E., et al. 2000, ApJ, 532, 170
Stern, D., Yost, S. A., Eckart, M. E., et al. 2005, ApJ, 619, 12
Tilvi, V., Rhoads, J. E., Hibon, P., et al. 2010, ApJ, 721, 1853
van Breukelen, C., Jarvis, M. J., & Venemans, B. P. 2005, MNRAS, 359, 895
Willis, J. P., Courbin, F., Kneib, J.-P., & Minniti, D. 2008, MNRAS, 384, 1039
Yan, H., Finkelstein, S. L., Huang, K.-H., et al. 2012, ApJ, 761, 177
Yan, H.-J., Windhorst, R. A., Hathi, N. P., et al. 2010, RAA, 10, 867